# Tailoring of Stress Development in MEMS Packaging Systems

Satyajit S.Walwadkar and Junghyun Cho
Dept. of Mechanical Engineering, State University of New York, Binghamton, NY 13902-6000;

P.W. Farrell and Lawrence E. Felton
Analog Devices, Micromachined Product Division, 21 Osborn Street, Cambridge, MA 02154

## ABSTRACT

A better understanding of the origin and evolution of the stresses is a crucial step in improving reliability of packaging systems for microelectromechanical systems (MEMS). Given its importance, we examine the stresses developed in hermetically packaged MEMS inertial sensors. For this purpose, an optical surface profilometer is employed to assess the stresses by measuring the curvature of dummy silicon dies (3.5x3.5 $mm^2$) assembled in different types of packages and die attach adhesives. We also explore a temporal evolution of stresses during thermal exposure of the test packages in an effort to emulate actual packaging processes and device operation conditions. The result shows different levels of stresses generated from various adhesives and package types, and also a stress evolution during packaging processes. The mechanical stress data also show a good agreement with MEMS performance data obtained from actual accelerometers. Therefore, the stress data will not only be useful in better understanding performance of MEMS packages, but the testing protocol can also provide a diagnostic tool for very small packaging systems.

## INTRODUCTION

MEMS technology integrates mechanical elements, sensors, actuators and electronics onto a common substrate by applying so called microfabrication that is similar to the CMOS fabrications in microelectronic industry. The technological developments in this field have rapidly advanced and diversified in the past few years [1-4]. In particular, silicon based inertial sensors such as accelerometers and gyroscopes have widely been used in navigation, automotive, consumer, military, and seismic markets [5-7]. For example MEMS inertial sensors are quickly replacing conventional air-bag deployment systems in automobiles [8]. Importantly, they become much smaller and cheaper, but provide more functionality, and are reliable to use.

However, packaging of the MEMS devices and systems needs to be improved to a great extent from its current stage. Presently, nearly all the MEMS packaging efforts must develop a new specialized package each time a new device is designed. In addition, the MEMS packaging presents unique challenges compared to the IC counterpart due to the diversity of MEMS devices and the requirement that many of these devices be in a continuous and intimate contact with their environment. It is not unusual that the packaging content is responsible for 75% to 95% of the overall cost of MEMS devices [9].

The package should also be free from residual stresses that are developed during the course of the packaging processes, followed by thermal cycling environment [10]. Therefore, it is essential to understand the origin and evolution of the stresses in order to improve the reliability of the MEMS packaging systems. Another effect from the stresses in the packaging is a long-term drift resulting from slow creep in the adhesive that attaches the silicon die to the substrate.

Given that, the main focus of this work is to examine a stress development in hermetically packaged MEMS devices. The Wyko optical profilometer with a vertical scanning capability is used to measure the die warpage (curvature; out-of-plane displacement) resulting from different heat treatments and material systems [11]. This technique has a capability to scan a wide range of height information from about 0.1 nm to 500 μm, whose feature is useful in die warpage measurement.

## EXPERIMENTAL PROCEDURE

In an attempt to identify a stress testing protocol for relatively small silicon dies, we employed a non-contact, optical profilometer that employs a light interference to measure the warpage of the die by tracing its surface profile. From the theory of elasticity, it is known that the stresses at a point in a thin plate due to bending moments can be expressed in terms of the local curvature of the plate as given by:

$$\sigma_x = \frac{Et(1/R_x + \nu/R_y)}{(1-\nu^2)}, \quad \sigma_y = \frac{Et(1/R_y + \nu/R_x)}{(1-\nu^2)} \qquad (1)$$

where $E$ is Young's modulus, ν is Poisson ratio, $t$ is a half of the thickness of the plate, and $R_x$ and $R_y$ are the radius of curvature in the x- and y-direction, respectively [12,13].

This instrument uses interferometric technique along with the digital signal processing algorithms to produce accurate, repeatable 3-dimensional surface profiles. We used scanning white light interferometry (SWLI), in which an incoming light is split onto an internal reference surface and a silicon die surface (Fig. 1). After reflection, the light beams recombine inside the interferometer, thereby undergoing constructive and destructive interference and producing light and dark fringe patterns [14].

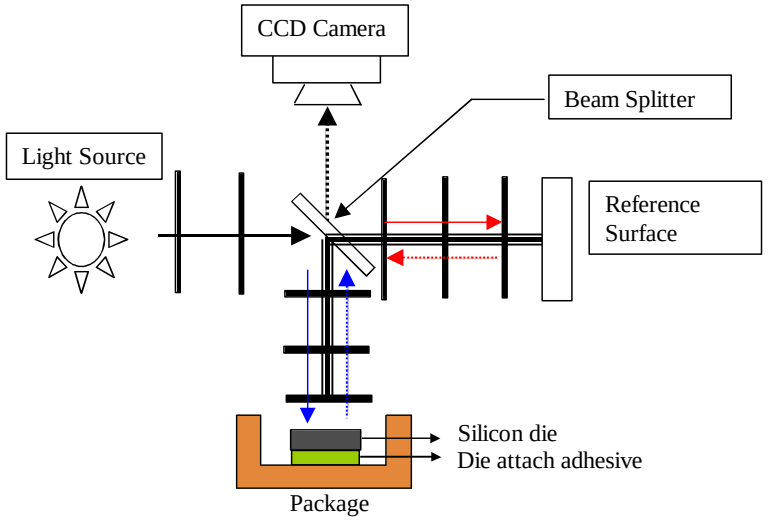


**Figure 1.** Operational principle of a Wyko optical profilometer used in this study along with a stress testing package.

Surfaces of the dummy silicon dies (3.5x3.5 $mm^2$) in the ceramic packages were profiled for stress testing. Three different die attach adhesives (silver glass, polyimide, silicone) were used to assemble the die into different types of ceramic packages. For a reference, bare silicon dies, which were cut from the silicon wafers, were also examined before die attach for an initial warpage measurement. Table 1 summarizes the test packages and adhesives used in this study.

**Table 1.** Summary of package types and adhesives employed in this study.

| Package types | Package variations | Adhesives for die attach |
|---|---|---|
| Ceramic plate (CP) | Type A (PKG CP-A)<br>Type B (PKG CP-B) | Silver glass<br>Polyimide<br>Silicone |
| Sidebraze (SB) | Type A (PKG SB-A)<br>Type B (PKG SB-B) | Silver glass<br>Polyimide<br>Silicone |
| Ball-grid array (BGA) | Type A (PKG BGA-A)<br>Type B (PKG BGA-B)<br>Type C (PKG BGA-C)<br>Type D (PKG BGA-D) | Silver glass<br>Polyimide<br>Silicone |

These packages were further tested to understand a temporal evolution of the stresses during thermal exposure of the test packages, which emulates actual packaging processes and device operating conditions. Figure 2 shows heat treatment conditions employed for the stress testing packages and the stress measurement schedules. All the measurements were performed at room temperature, and each sample was measured twice (non consecutively).

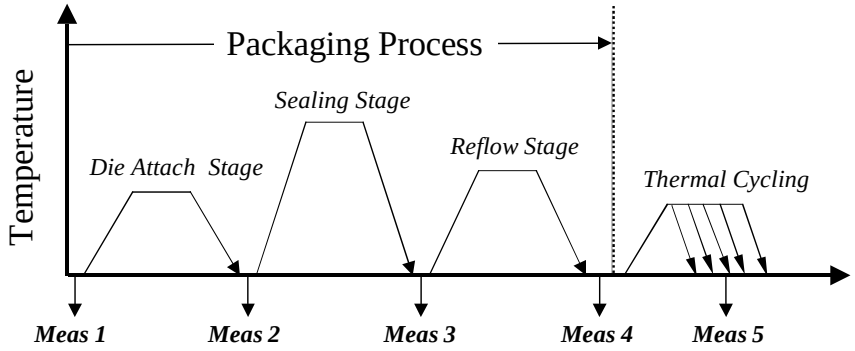


| Packaging Process / Post Operation | Corresponding Experimental Condition |
|---|---|
| Die attach | **Silver glass**: cured at peak temp of 355˚C<br>**Polyimide**: cured at 100˚C for 30 min and 200˚C for 30 min<br>**Silicone**: cured at 150˚C for 60 min in $N_2$ atmosphere |
| Solder sealing for package lid attachment | Peak temp at 340˚C, 60˚C/min ramp rate |
| Solder reflow for board attach | Peak temp at 240˚C |
| Thermal cycling | Between –55˚C to 125˚C |

**Figure 2.** Standard packaging processes followed by thermal cycles and corresponding heat treatments used in this study for the stress measurement.

## RESULTS AND DISCUSSION

Figure 3a shows a 3-dimensional surface profile of a silicon die attached to the substrate. As seen here, a dome-shaped surface profile was found, indicating the warpage. The profile was acquired after the test package was die attached and heat treated for a solder sealing process. In order to estimate the warpage (curvature), a line profile across both x-direction and y-direction was drawn as shown in Fig. 3b. Most of surface profiles obtained from this study show uniform stress distribution (circular-dome shape), but non-uniform, elongated warpage shapes were also observed.

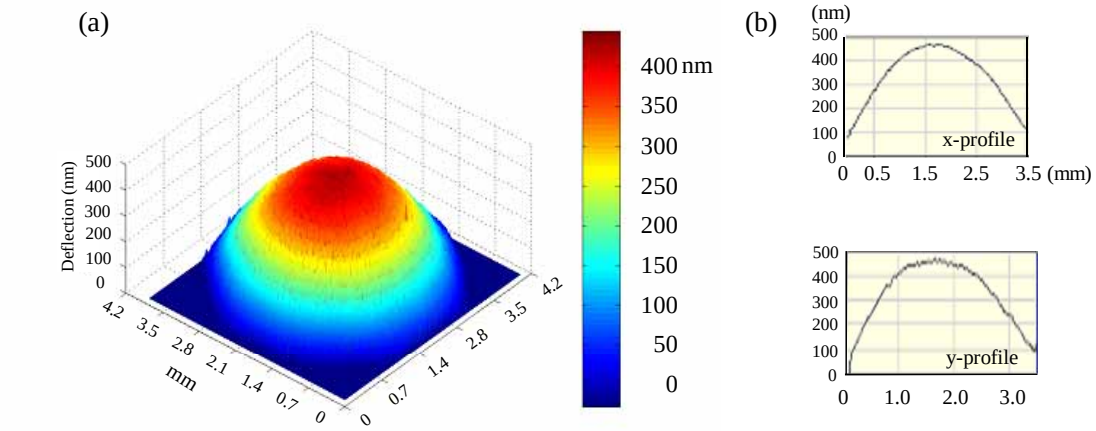


**Figure 3.** (a) 3-dimensional surface profile of a silicon die in PKG SB-A assembled with a silver glass adhesive; (b) x- and y-line profile across the die.

In order to test a performance of different adhesives, we measured the stresses of the dies assembled from these adhesives using the ceramic plate (Fig. 4a). Both x- and y-line profiles were obtained. As shown here, bare dies tested in this study showed a certain level of warpage at the initial stage. A significant increase in the warpage was observed right after die-attach and sealing processes except for the packages assembled with the silicone adhesives, indicating that most of the stresses are induced at these stages due to shrinkage of die attach adhesives during curing. Similarly, MEMS performance data also indicate that the package with the silicone has a smallest standard deviation in accelerometer output (Fig. 4b). According to the stress deflection data, the polyimide adhesives showed a better performance than the silver glass, while the former showed slightly a higher deviation than the latter in the MEMS output performance. The calculated stress range in Fig.4a varies from about 5 to 80 MPa.

It should be noted that there exists manufacturing variation in each package, partly because of the die attach process and control (e.g., thickness and spatial uniformity of adhesives, temperature variation, etc.). In addition to the different adhesive types, various package types were compared for each adhesive by exposing the same sample in a series of heat treatments (Fig. 5). It shows a large deviation among different package types, but still indicate a best performance by the silicone adhesives. Interestingly, the polyimide adhesive displays a slightly higher stress value than the silver glass in some package types (at a sealing stage), which is in fact consistent with the above MEMS performance data as shown in Fig. 4b.

One interesting observation here is that both types of packages using the silver glass adhesive showed a gradual decrease in the stresses after die attach (Fig. 5a), while the other two

adhesive cases did not show this behavior. It clearly suggests that there is a stress relaxation mechanism for the silver glass adhesive. Further studies are required to understand this behavior better.

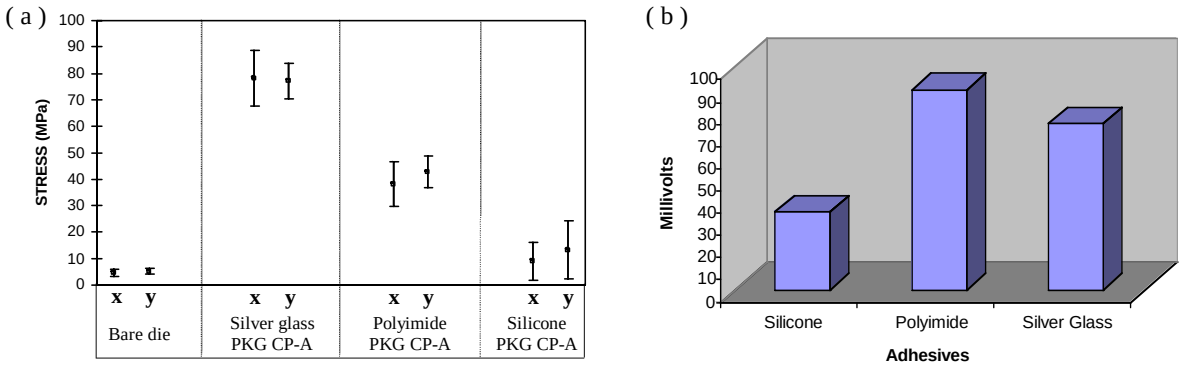


**Figure 4.** (a) Out-of-plane displacement data from different adhesives, as compared to those from bare dies. The error bar represents for the standard deviation of an average value of 3-5 samples. (b) Accelerometer output standard deviation for these adhesive types after packages were sealed with a top lid.

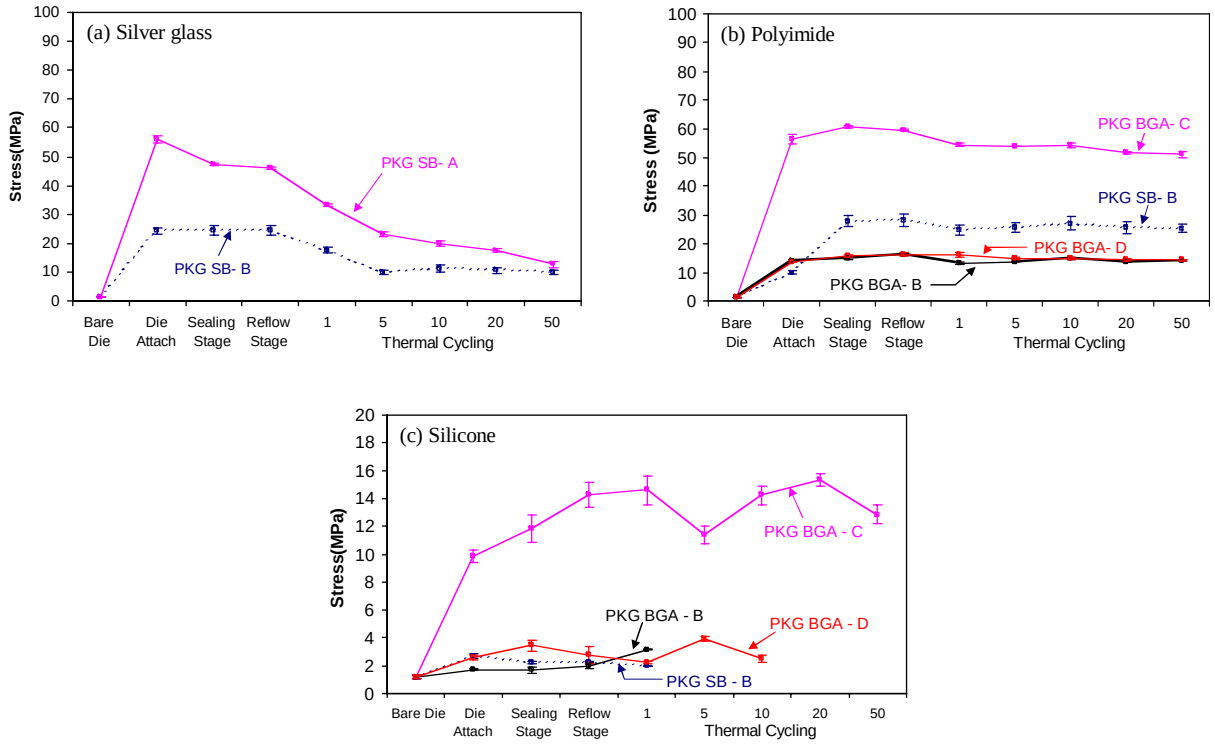


**Figure 5.** Performance comparison during heat treatments among different package types for (a) silver glass, (b) polyimide, and (c) silicone. The error bar represents for a data scattering (between x- and y-directions) of each sample.

## CONCLUSIONS

This study demonstrates a potential of an optical profilometer in measuring small amounts of stresses developed in small-scale devices. Among different types of adhesives compared, it was shown that the silicone outperforms the other two types of adhesives in terms of the stress developed in the die. This trend is consistent with the accelerometer output data, but more work is needed to have a correlation between the stress levels and MEMS performance. Even with the same type of adhesive, there exist a stress variation among different package types. Therefore, it is of great importance to select a right combination of a die attach adhesive and a package type to minimize the stress development. When mimicking the actual packaging processes, most of the stresses were developed right after the die attach process.

It was also shown that the stress is gradually decreased for the silver glass adhesives as a function of packaging processes, whose behavior is not observed for the polyimide and silicone adhesives. There must exist a stress relaxation mechanism in the silver glass, and more systematic studies are currently underway. Overall, the resultant stress data showed a good agreement with MEMS accelerometer performance data, suggesting that the stress data be used as a guide to determine the device performance.

## ACKNOWLEDGMENTS

This research was funded by Analog Devices, Inc. and Integrated Electronics Engineering Center (IEEC) at State University of New York at Binghamton.

## REFERENCES

1. S.M. Spearing, Acta Mater, **48**,179-196 (2000).
2. J.J. Sniegowski and M.P. de Boer, Ann. Rev. Mater. Sci., **30**, 299-333 (2000).
3. A.Y. Tonkovich, C.J. Call, D. Jimenez, R.S. Wegeng, and M.K. Drost, Heat Transfer-Houston 1996, **310**, 119-125 (1996).
4. Li Cao, S. Mantell and D. Polla, Sensors and Actuators A, **94 [1-2]** 117-125 (2001).
5. T.A. Core, W.K. Tsang and S.J. Sherman, Solid State Technology, **36 [10]** 39-44 (1993).
6. T. Tsuchiya, Y. Kageyama, H. Funabashi, and J.Sakata, Sensors and Actuators A, **90**, 49-55 (2001).
7. F. Ayazi, J. Microelectromechanical System, **10 [2]** 169-79 (2001).
8. L. Zimmermann, J.P. Ebersohl, F.L. Hund, J.P. Berry, F. Baillieu, P. Rey, B. Diem, S. Renard, P. Caillat, Sensors and Actuators A, **46-47**, 190-95 (1995).
9. N. Maluf, An Introduction to Microelectromechanical Systems, Artech House, Inc., Norwood, MA, 2000.
10. P.H. Tsao and A.S. Voloshin, IEEE Trans. Comp. Packag. and Manufact. Tech. A, **18 [1]** 201-205 (1995).
11. B. Bowe and V. Toal, Opt. Engn., **37 [6]** 1796-99 (1998).
12. J. W. Dally and W. F. Riley, Experimental Stress Analysis, 3rd ed., McGraw-Hill, Inc., New York, NY, 1991.
13. E. E. Sechler, Elasticity in Engineering, Dover Publications, Inc., New York, NY, 1968.
14. M. Hill, C. O'Mahonya, H. Berneya, P.J. Hughesa, E. Hynesb, and W.A. Lanea, Opt. and Lasers in Engn., **36**, 169-183 (2001).